Status and perspectives with exotic states at LHCb

Results and prospects

A. Augusto Alves Jr, on behalf of the LHCb collaboration.

University of Cincinnati
aalvesju@cern.ch

LHC SKI 2016, A first discussion of 13 TeV results,
10-15 April 2016, Obergurgl

Outline

1. The LHCb detector
2. Exotic states
3. Results on $P(4380)^+_c$
4. Results on $Z(4430)^+$
5. Discussion

The LHC environment

During most of 2012 run, LHC collided protons at 8 TeV with an average instantaneous luminosity of $4 \times 10^{32} cm^{-2} s^{-1}$ (LHCb) and 20 MHz of bunch crossing.

- Inelastic cross section $\sim 60\,\mathrm{mb}$
- $\sigma(\mathrm{pp} \to \mathrm{b\bar{b}}X) = (284 \pm 20(\mathrm{stat}) \pm 49(\mathrm{syst}))\ \mu\mathrm{b}$ [PLB 694, 209]
- $\Longrightarrow$ $\sim 10^6$ $\mathrm{B\bar{B}}$ produced per second
- $\sigma(\mathrm{pp} \to c\bar{c}X)$ is about 20 times higher. [Nucl.Phys. B871 (2013) 1-20]

At the LHC energy, the $\mathrm{b\bar{b}}$ pairs are produced preferentially at forward (backward) directions.

- Optimal design is a forward detector: LHCb

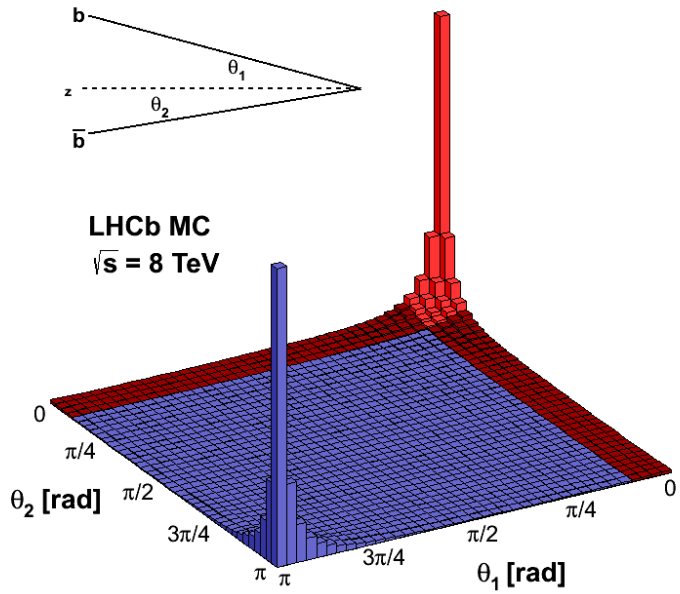

The LHCb detector

LHCb experiment was designed to perform high precision flavour physics measurements at the LHC.

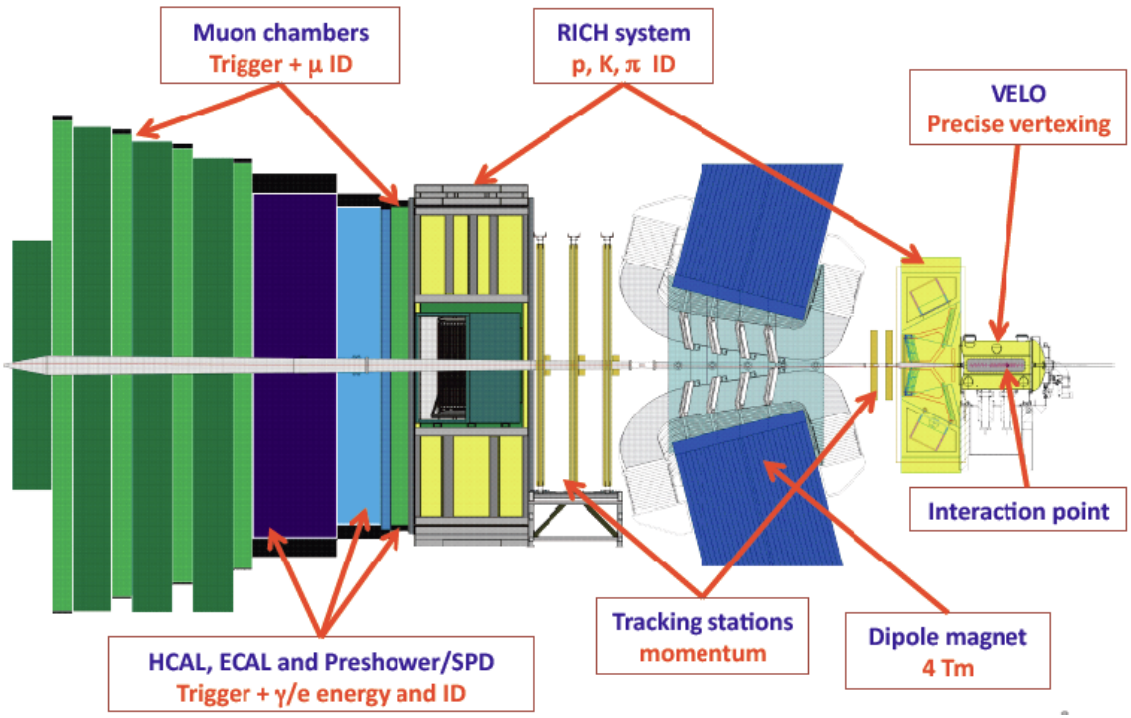

- **Single-arm design.** Covering the range $2 < \eta < 5$, LHCb can exploit the dominant heavy flavour production mechanism at the LHC and detects $\sim$ 40% of the $\mathrm{b\bar{b}}$ produced in forward region.
- **Good particle identification.** Excellent muon identification and good separation of π, K and p over (2 - 100) GeV.

- **Good vertexing and tracking.** Precise primary and secondary vertex reconstruction. Excellent momentum, IP and proper time resolution.
- These same features make LHCb very suitable for precision spectroscopy studies in the foward region.

The LHCb detector

Runs I and II

	Run I (2011 + 2012)	Run II (2016)
Bunch spacing	50ns	25ns
E_{cm}	7 TeV / 8 TeV	13 TeV
Luminosity	$1 + 2$ fb^{-1}	>5 fb^{-1}
Bunches	up to 1262	$\sim$2622

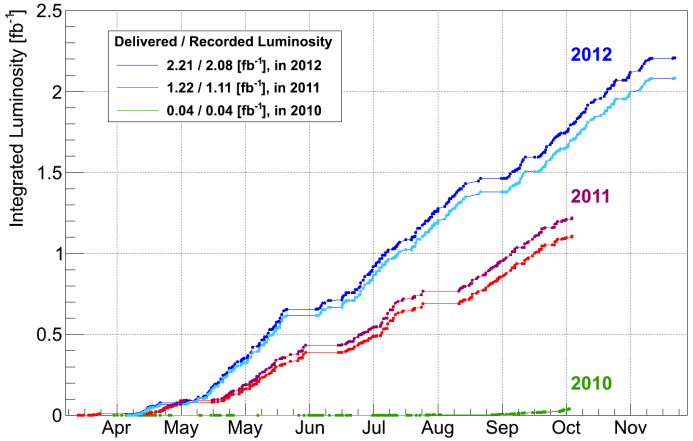

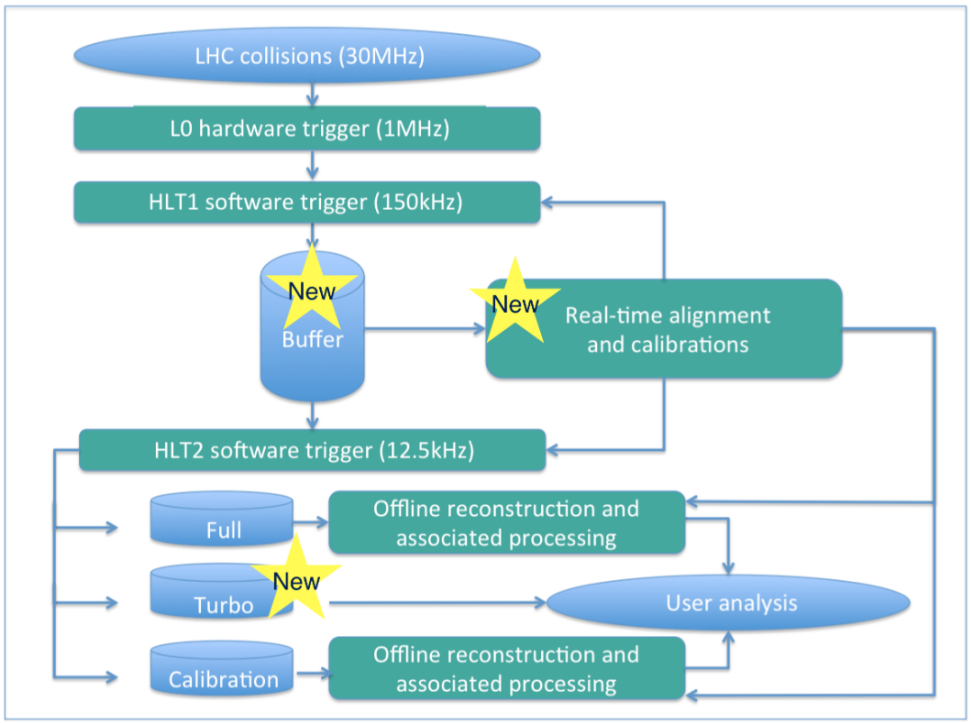

- The calibration and alignment process takes place now automatically online.
- The stored data are immediately available offline for physics analysis (turbo stream).
- The "turbo" data sample keeps only information necessary to perform physics analysis with the offline quality
- See the Barbara's talk after the coffee break.

XYZ states

Many new states have been observed at Charm, b-factories and Tevatron

- Masses lying on the limits of the quarkonia spectrum
- Observed many different production mechanisms: ISR, e^+e^-, $\gamma\gamma$ and B decays.
- The measured masses do not correspond to the predicted values for conventional quarkonia.
- The properties do not fit very well to the quarkonia picture.

Many theoretical interpretations in discussion:

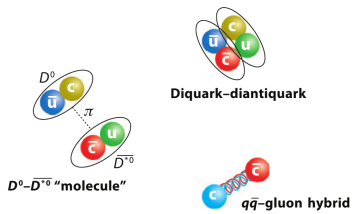

- conventional quarkonia;
- multiquark states;
- meson-molecules;
- hybrid mesons;
- threshold effects;

The table should be updated to include some new states: $P(4380)^+_c$, $P(4450)^+_c$ ...

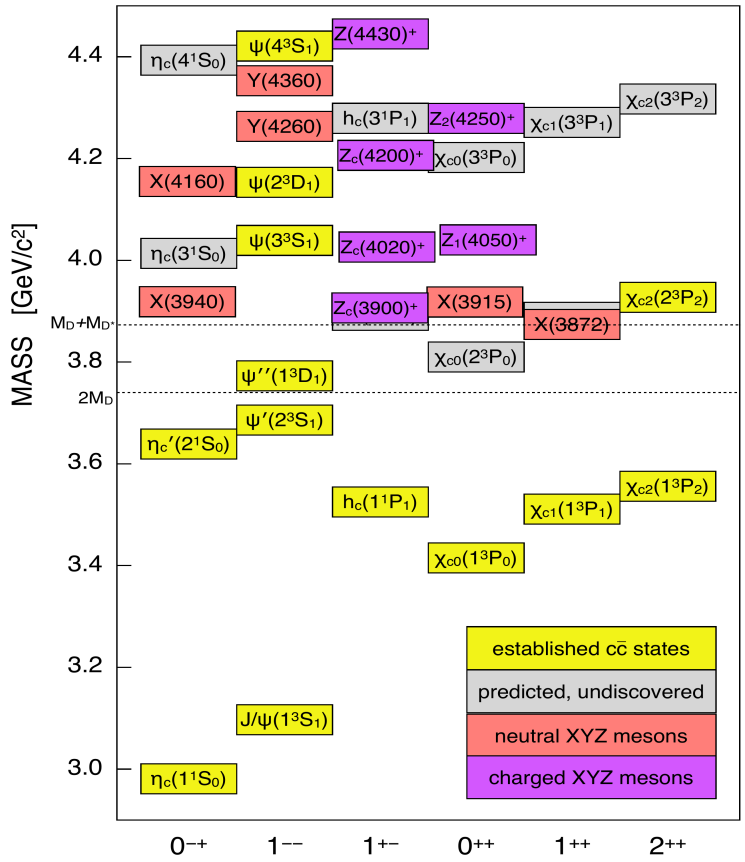

[PoS Bormio 050(2015) arXiv:1511.01589]

$\Lambda_b^0 \to K^- p J/\psi$

Phys. Rev. Lett. 115 (2015) 072001

- Sample with >26.000 $\Lambda_b^0 \to K^- p J/\psi$ signal candidates,
- Analysis: six-dimensional amplitude fit (invariant masses, helicity and decay planes angles).
- Background from sidebands. Estimated 5.4% of combinatorial background in the signal region.
- Six-dimensional efficiency calculated using complete simulation of the detector

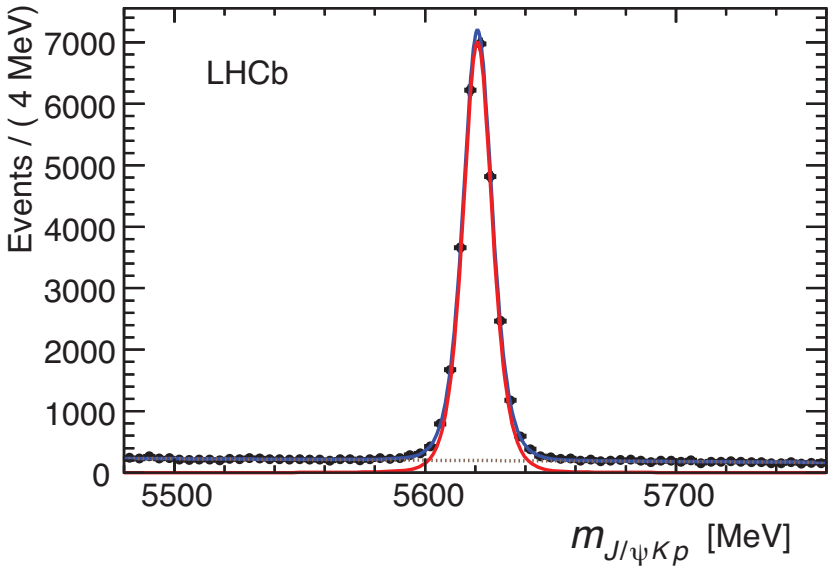

background subtracted Dalitz plot

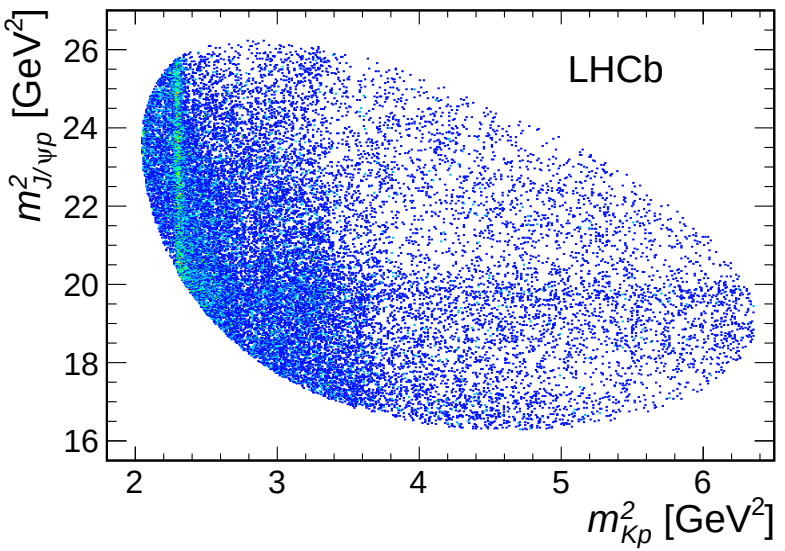

$\Lambda_b^0 \to K^- p J/\psi$

Some analysis details

- Two parametizations: $\Lambda_b^0 \to K^- (P_c^+ \to p J/\psi)$ and $\Lambda_b^0 \to J/\psi (\Lambda^* \to p K^-)$, with $J/\psi \to \mu^+ \mu^-$

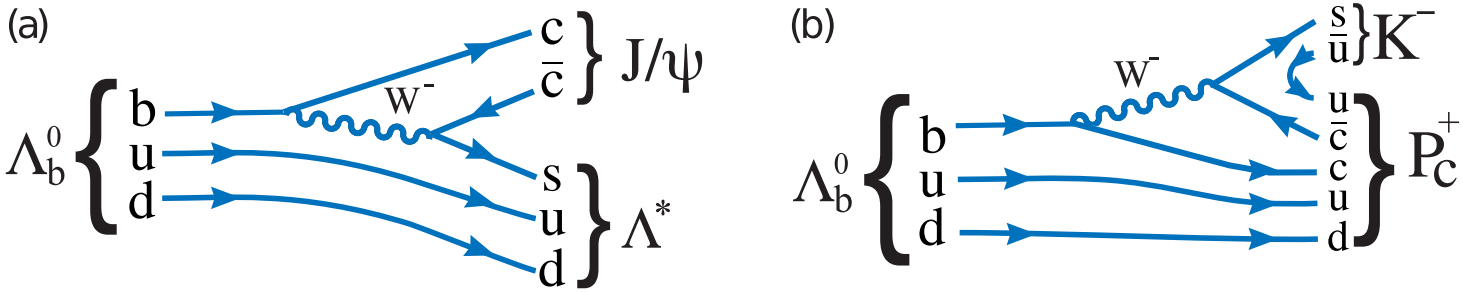

- Six-dimensional amplitude fit. Resonance invariant mass, three helicities angles, and two differences between decay planes.

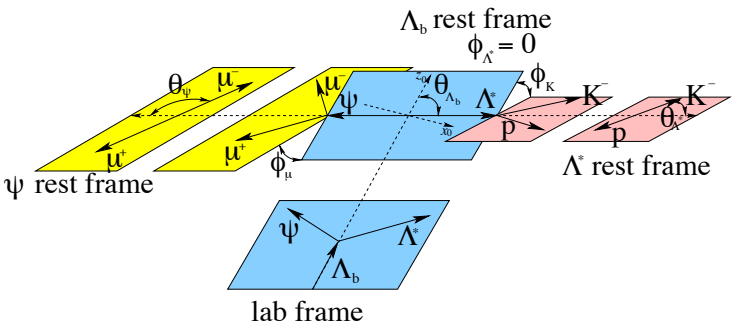

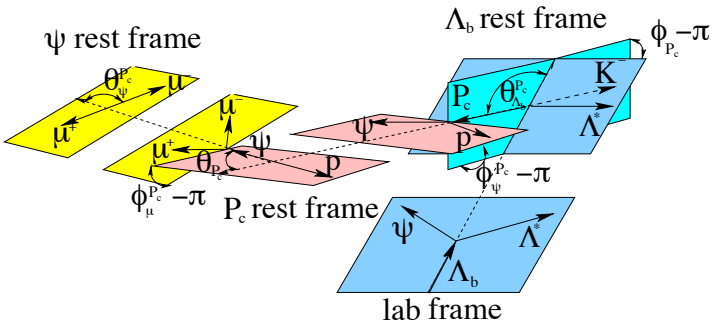

- Lorentz transformations relates the two helicity representantions.
- Resonances described by Breit-Wigner.
- Angular distribution calculated using helicity formalism.

$\Lambda_b^0 \to K^- p J/\psi$

Fit results with pentaquark states

- Fit including just well motivated Λ^* resonances (Reduced model).
- Two P_c^+ states necessary to achieve acceptable fit quality.
- $P(4380)_c^+$ with $M = 4380 \pm 8 \pm 29\,\mathrm{MeV}/c^2$ and $\Gamma = 205 \pm 18 \pm 86\,\mathrm{MeV}/c^2$ $J^P = 3/2^-$, fit fraction of $(8.4 \pm 0.7 \pm 4.2)\%$ and significance of 9σ
- $P(4450)_c^+$ with $M = 4449.8 \pm 1.7 \pm 2.5\,\mathrm{MeV}/c^2$ and $\Gamma = 39 \pm 5 \pm 19\,\mathrm{MeV}/c^2$ $J^P = 5/2^+$, fit fraction $(4.1 \pm 0.5 \pm 1.1)\%$ and significance of 12σ
- The mass resolution is approximately $2.5\,\mathrm{MeV}/c^2$ and combined significance 15σ

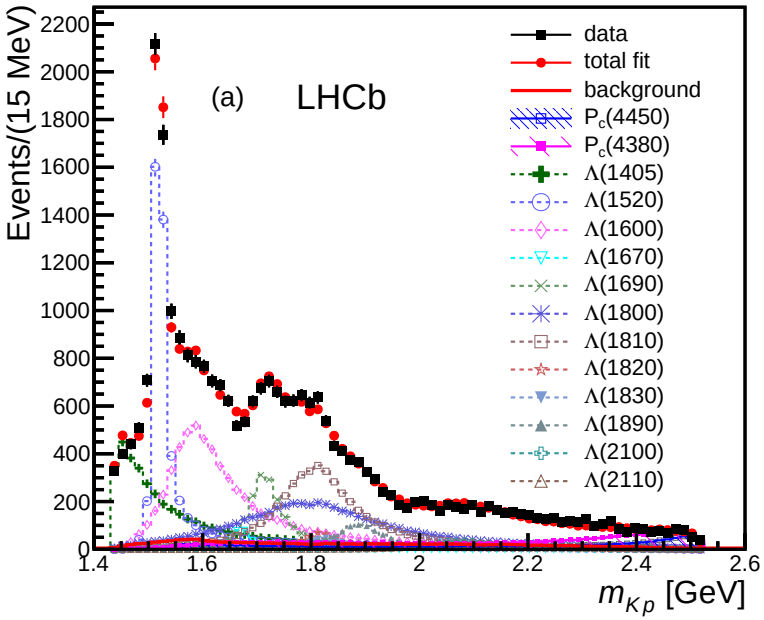

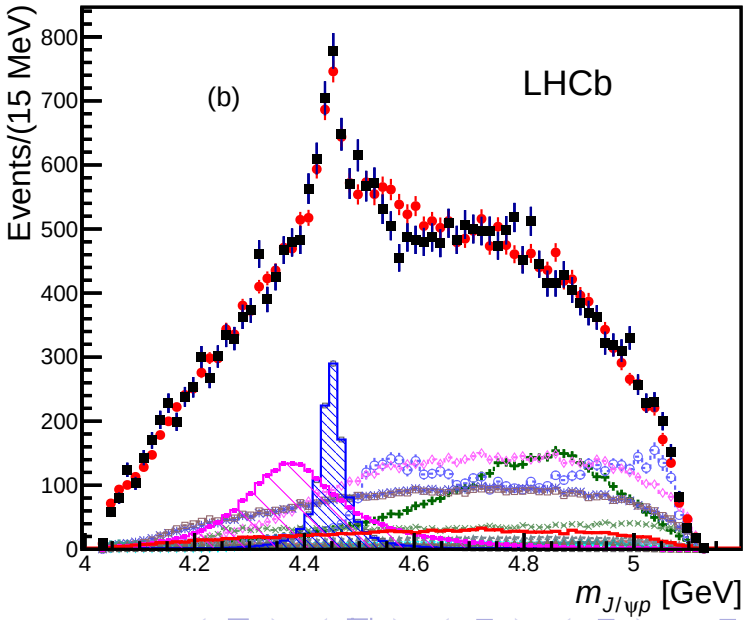

$\Lambda_b^0 \to K^- p J/\psi$

Resonant character of the pentaquark state

- $P(4450)_c^+$ amplitude is now described by 6 independent complex numbers instead of a Breit-Wigner
- Six equidistant points in the range $\pm\Gamma_0 = 39\,\mathrm{MeV}/c^2$ around $M_0 = 4449.8\,\mathrm{MeV}/c^2$ (from the default fit)
- Observe a fast change of phase crossing maximum of magnitude. Expected behavior for a resonance.
- Same test on $P(4380)_c^+$ leads to inconclusive results

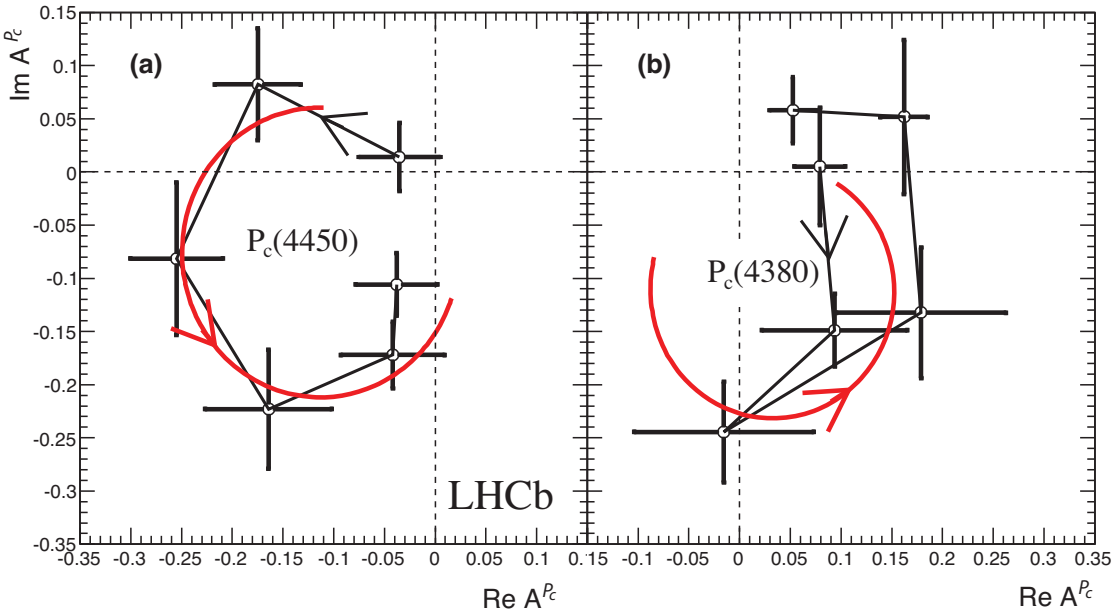

Confirmation of $Z(4430)^+$ at LHCb

Phys.Rev.Lett.112, 222002 (2014)

- Sample with >25.000 $B^0 \to K^+\pi^-\psi(2S)$ signal candidates,
- Analysis performed using two different approaches:
  - Model dependent. Four-dimensional amplitude fit (invariant masses, helicity and decay planes angles).
  - Model independent. An analysis based on the Legendre polynomial moments extracted from the $K\pi$ system
- Background from sidebands. Estimated 4% of combinatorial background in the signal region.
- Four-dimensional efficiency calculated using complete simulation of the detector

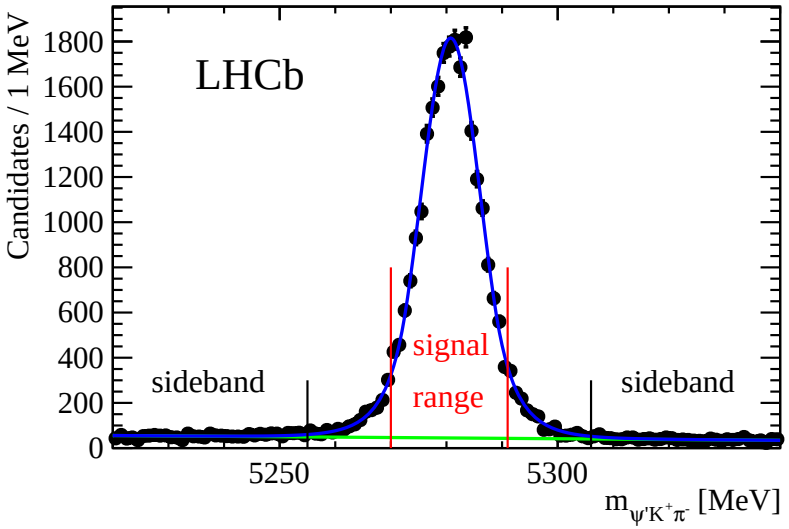

background subtracted Dalitz plot

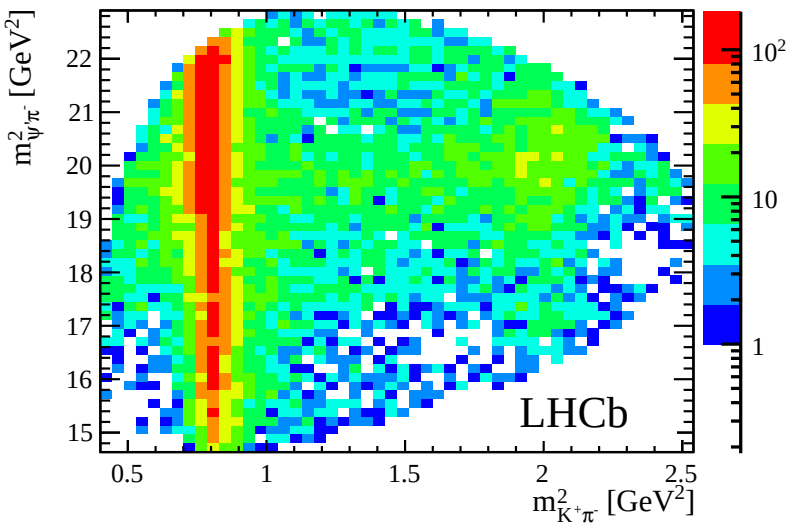

$Z(4430)^+$
Amplitude fit

- Fitted parameters:

$$M_{Z(4430)^+} = 4475 \pm 7^{+15}_{-25}\,\mathrm{MeV}/c^2, \Gamma_{Z(4430)^+} = 172 \pm 13^{+37}_{-34}\,\mathrm{MeV}/c^2$$

$$f_{Z(4430)^+} = (5.9 \pm 0.9^{+1.5}_{-3.3})\%$$

.

- Significance: $\Delta(-2lnL) > 13.9\sigma$

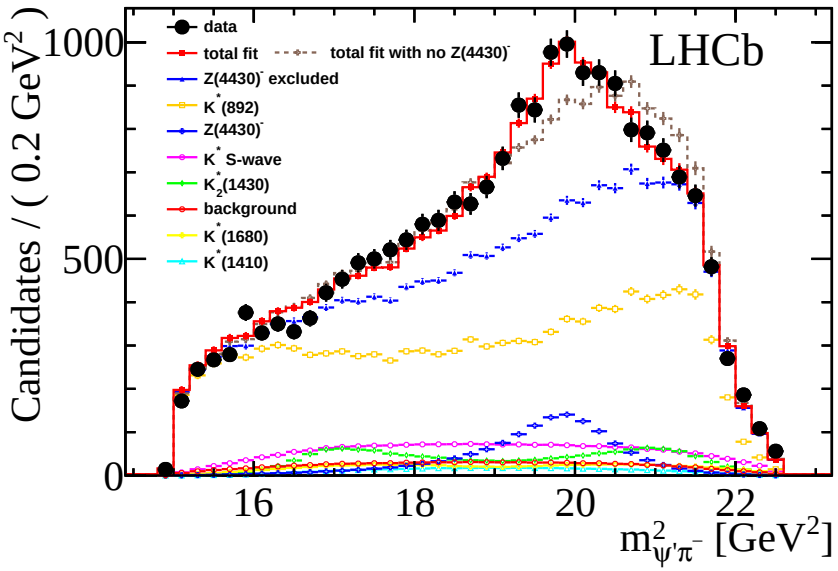

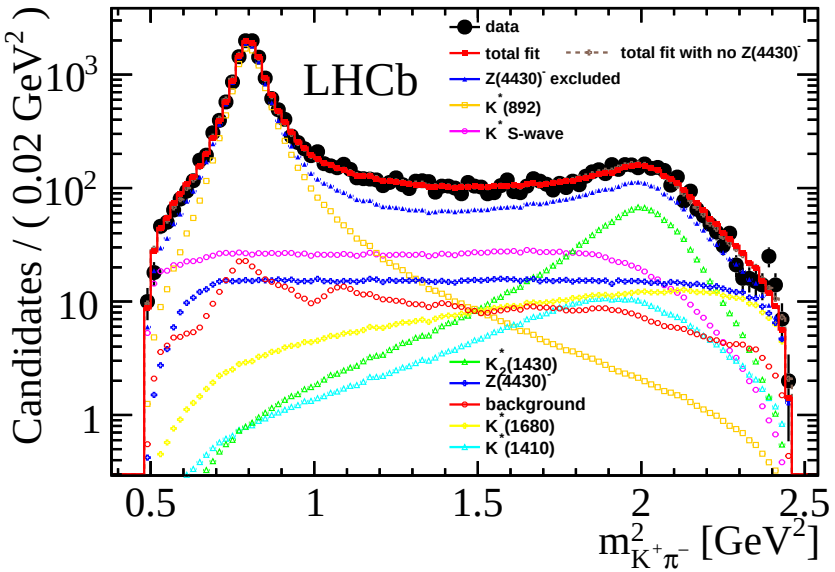

$Z(4430)^+$

Resonance character and spin determination

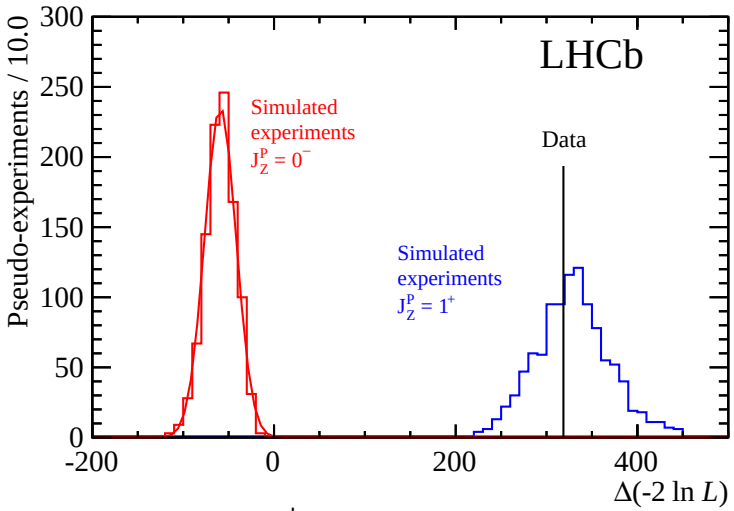

- $J^P = 1^+$ assignment favored.
- Other J^P assignments are ruled out with large significance: $> 9\sigma$

- $Z(4430)^+$ amplitude is described by 6 independent complex numbers instead of a Breit-Wigner
- Observe a fast change of phase crossing maximum of magnitude.
- Expected behaviour for a resonance.

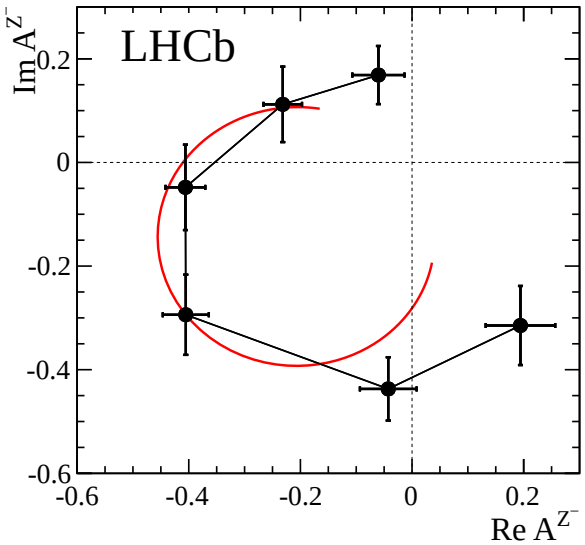

$Z(4430)^+$: model independent analysis

Phys. Rev. D 92, 112009 (2015)

- Very active $\mathrm{K}\pi$ system.
- $\mathrm{m}_{\mathrm{K}\pi}$ taken directly from data, as it is.
- Angular structure of the $\mathrm{K}\pi$ system acquired via Legendre polynomials.
- $\frac{dN}{d\cos\theta_{K^{*0}}} = \sum_{j=0}^{l_{max}} \langle P_j^U \rangle \mathrm{P}_j(\cos\theta_{K^{*0}})$
- $\langle P_j^U \rangle = \sum_{i=1}^{N_{reco}} \frac{W^i_{signal}}{\epsilon^i} \mathrm{P}_j(\cos\theta^i_{K^{*0}})$

Resonance	Mass (MeV/c^2)	Γ (MeV/c^2)	J^P
$K^*(800)^0$	682±29	547±24	0^+
$K^*(892)^0$	895.81±0.19	47.4±0.6	1^-
$K^*(1410)^0$	1414±15	232±21	1^-
$K_0^*(1430)^0$	1425±50	270±80	0^+
$K_2^*(1430)^0$	1432.4±1.3	109±5	2^+
$K^*(1680)^0$	1717±27	322±110	1^-
$K_3^*(1780)^0$	1776±7	159±21	3^-

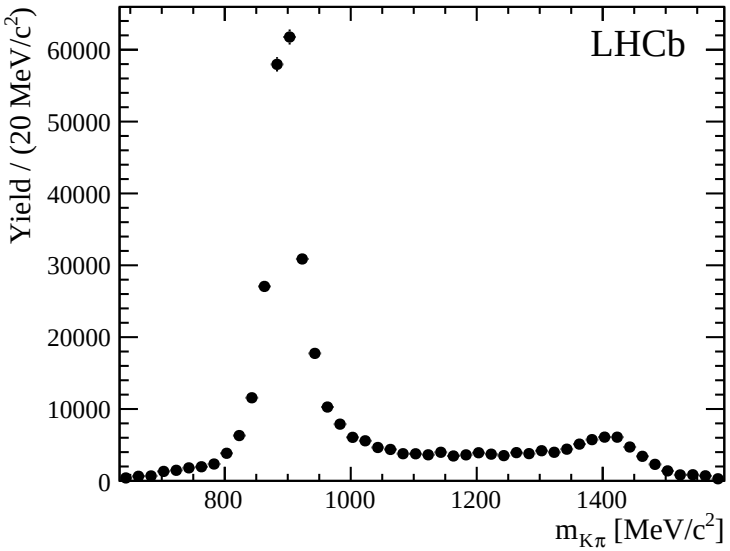

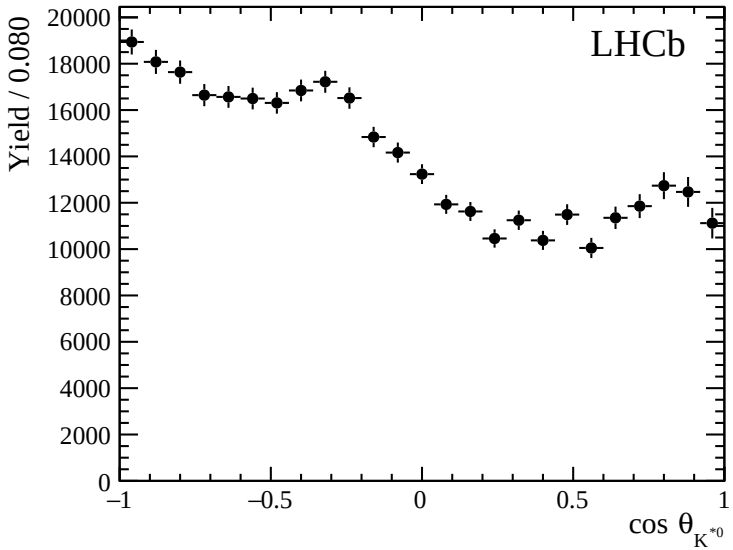

$Z(4430)^+$: model independent analysis

Legendre polynomial moments

The rich angular structure of the $K\pi$ system is shown by the very featured Legendre polynomial moments.

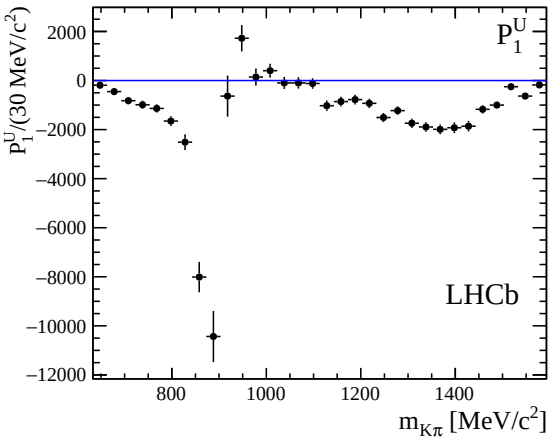

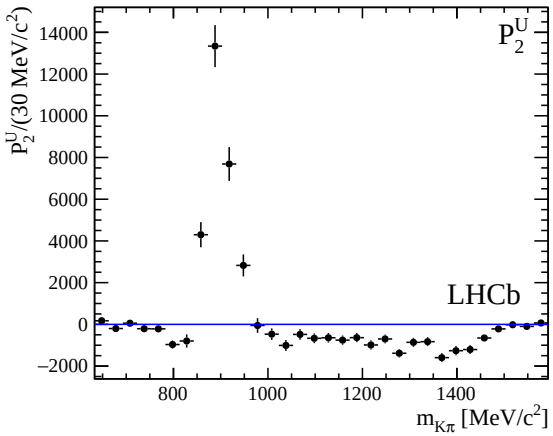

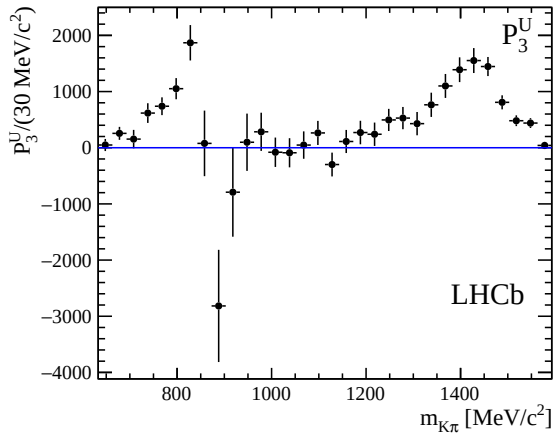

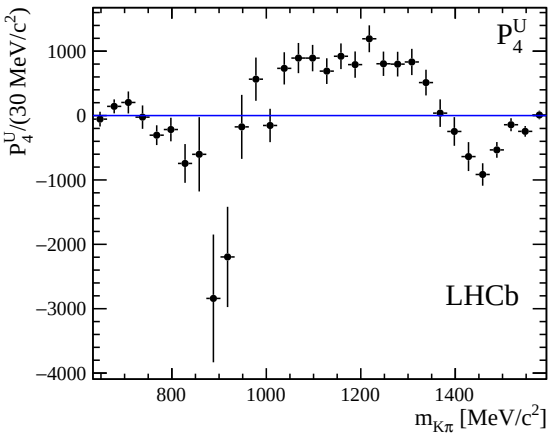

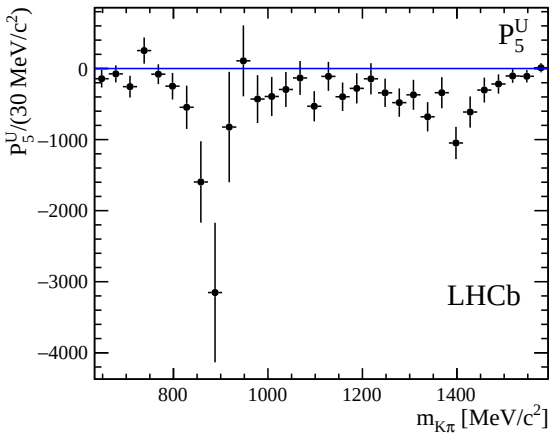

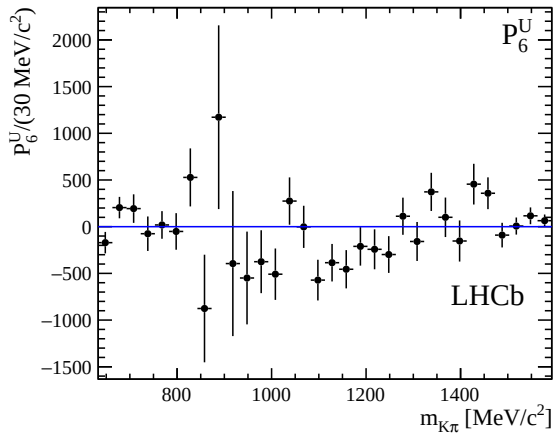

$Z(4430)^+$: model independent analysis

$m_{\psi(2S)\pi}$ spectrum

- The moments are normalized and used to predict, through a MC simulation, the expected $m_{\psi(2S)\pi}$ spectrum.
- The order of the Legendre polynomial expansion depends on the locally dominant $K\pi$ resonances

$$l_{\max}(m_{K\pi}) = \begin{cases} 2 & m_{K\pi} < 836\,\mathrm{MeV}/c^2 \\ 3 & 836\,\mathrm{MeV}/c^2 < m_{K\pi} < 1000\,\mathrm{MeV}/c^2 \\ 4 & m_{K\pi} > 1000\,\mathrm{MeV}/c^2. \end{cases}$$

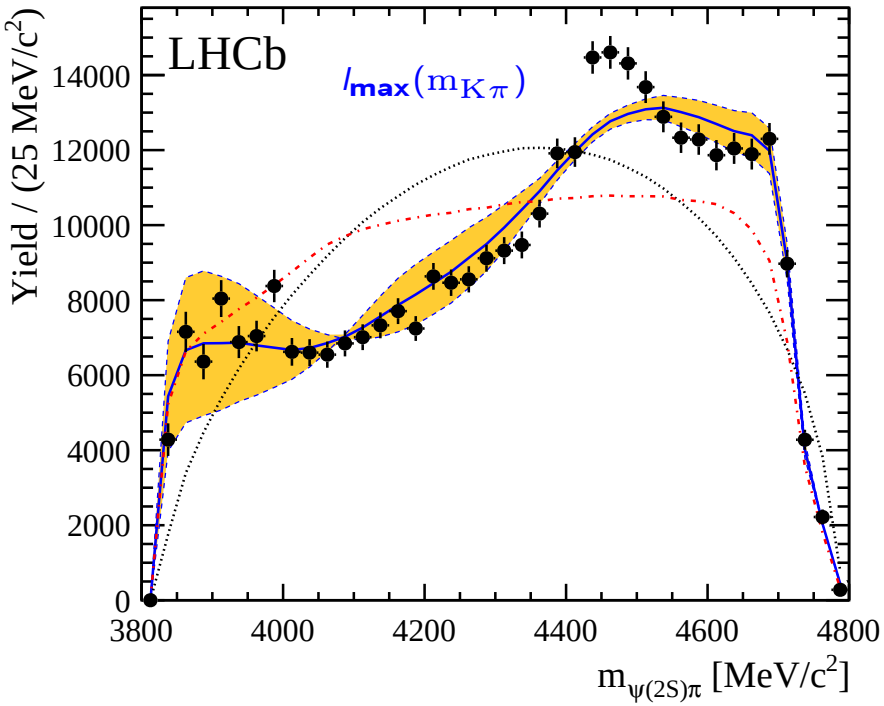

- **Data points(black dots)**
- **MC prediction (blue solid line)**
- Phase space MC (black dotted line)
- Phase space MC weighted to reproduce $m_{K\pi}$ (red line)

$Z(4430)^+$: model independent analysis

Hypothesis test

- Performed using a series of pseudo-experiments produced according with $l_{\max}$ $(m_{K\pi})$.
- Hypothesis test based on likelihood ratio between $l_{\max}$ $(m_{K\pi})$ and $l_{\max}$ =30.
- Efficiency effects and background subtraction taken into account in the pseudo-experiment generation.

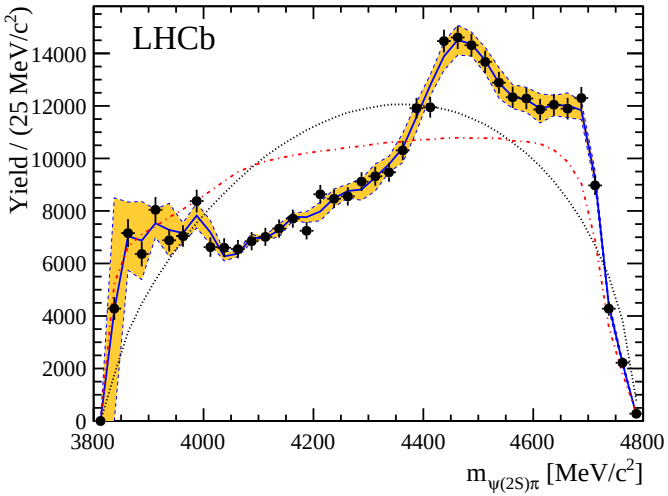

full $m_{K\pi}$ spectrum

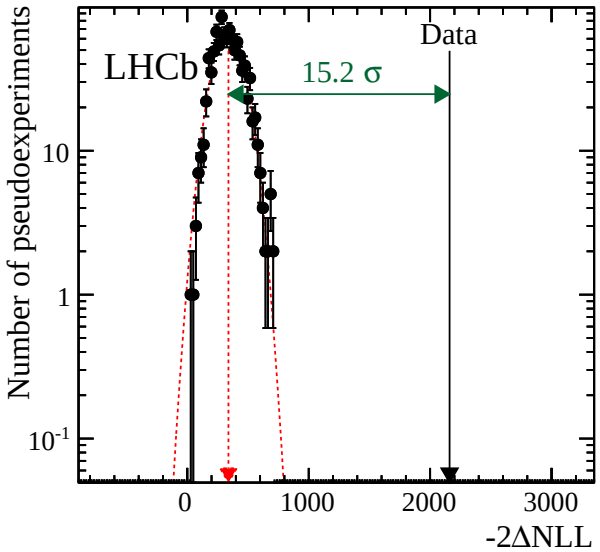

$1.0 < m_{K\pi} < 1.39\,\mathrm{GeV}/c^2$

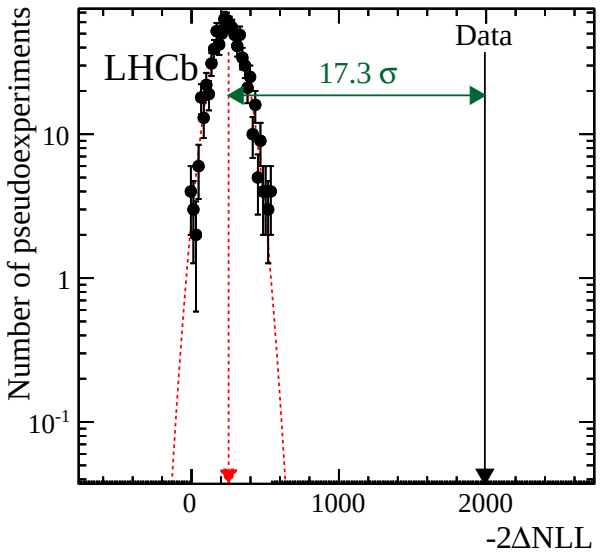

The hypotesis that the structure of the $m_{\psi(2S)\pi}$ spectrum can be described as a reflection of the activity of the resonances in the $K\pi$ system is ruled out with high significance.

Many other results in b and c spectroscopy

Access: http://lhcbproject.web.cern.ch/lhcbproject/Publications/LHCbProjectPublic/Summary_all.html

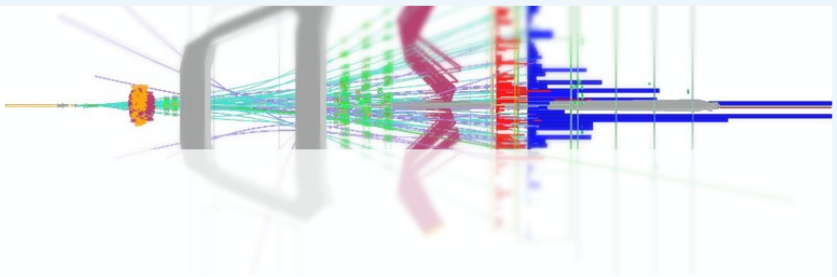

The LHCb Public results

LHCb publications

[to restricted-access page]

PUBLICATIONS PER WORKING GROUP

- FLAVOUR TAGGING
- b-HADRONS AND QUARKONIA
- B DECAYS TO CHARMONIUM
- DETECTOR PERFORMANCE
- CHARMLESS b-HADRON DECAYS
- QCD, ELECTROWEAK AND EXOTICA
- RARE DECAYS
- CHARM PHYSICS
- SEMILEPTONIC B DECAYS
- LUMINOSITY
- B DECAYS TO OPEN CHARM

List of papers (Total of 284 papers)

TITLE	DOCUMENT NUMBER	JOURNAL	SUBMITTED ON
Search for the rare decays $B^0 \to J/\psi\gamma$ and $B_s^0 \to J/\psi\gamma$	PAPER-2015-044	PRD	16 Oct 2015
Evidence for the strangeness-changing weak decay $\Xi_b^- \to \Lambda_b^0\pi^-$	PAPER-2015-047	PRL	13 Oct 2015
A model-independent confirmation of the $Z(4430)^-$ state	PAPER-2015-038	PRD	07 Oct 2015
Measurements of prompt charm production cross-sections in pp collisions at $\sqrt{s} = 13$TeV	PAPER-2015-041	JHEP	06 Oct 2015
Model-independent measurement of mixing parameters in $D^0 \to K_S\pi^+\pi^-$ decays	PAPER-2015-042	JHEP	06 Oct 2015
Measurement of the forward-backward asymmetry in $Z/\gamma^* \to \mu^+\mu^-$ decays and determination of the effective weak mixing angle	PAPER-2015-039	JHEP	25 Sep 2015
Studies of the resonance structure in $D^0 \to K_S^0K^\pm\pi^\mp$ decays	PAPER-2015-026	PRD	22 Sep 2015
Forward production of Υ mesons in pp collisions at $\sqrt{s} = 7$ and 8TeV	PAPER-2015-045	JHEP	08 Sep 2015
Measurement of forward J/ψ production cross-sections in pp collisions at $\sqrt{s} = 13$ TeV	PAPER-2015-037	JHEP	02 Sep 2015
First measurement of the differential branching fraction and CP asymmetry of the $B^\pm \to \pi^\pm\mu^+\mu^-$ decay	PAPER-2015-035	JHEP	01 Sep 2015
Measurement of CP violation parameters and polarisation fractions in $B_s^0 \to J/\psi\overline{K}^{*0}$ decays	PAPER-2015-034	JHEP	01 Sep 2015
Study of the production of Λ_b^0 and $\overline{B}^0$ hadrons in pp collisions and first measurement of the $\Lambda_b^0 \to J/\psi pK^-$ branching fraction	PAPER-2015-032	Chin Phys C	01 Sep 2015
Measurement of the time-integrated CP asymmetry in $D^0 \to K_S^0K_S^0$ decays	PAPER-2015-030	JHEP	25 Aug 2015
Search for hidden-sector bosons in $B^0 \to K^{*0}\mu^+\mu^-$ decays	PAPER-2015-036	PRL	17 Aug 2015
Measurement of the $B_s^0 \to \phi\phi$ branching fraction and search for the decay $B^0 \to \phi\phi$	PAPER-2015-028	JHEP	04 Aug 2015
B flavour tagging using charm decays at the LHCb experiment	PAPER-2015-027	JINST	28 Jul 2015
Measurement of the branching fraction ratio $\mathcal{B}(B_c^+ \to \psi(2S)\pi^+)/\mathcal{B}(B_c^+ \to J/\psi\pi^+)$	PAPER-2015-024	PRD	13 Jul 2015
Observation of $J/\psi p$ resonances consistent with pentaquark states in $\Lambda_b^0 \to J/\psi K^- p$ decays	PAPER-2015-029	Phys. Rev. Lett. 115 (2015) 072001	13 Jul 2015
Search for long-lived heavy charged particles using a ring imaging Cherenkov technique at LHCb	PAPER-2015-002	JHEP	30 Jun 2015
Angular analysis and differential branching fraction of the decay $B_s^0 \to \phi\mu^+\mu^-$	PAPER-2015-023	JHEP	29 Jun 2015

Summary

Established results

$P(4380)_c^+$ and $P(4450)_c^+$

- $P(4380)_c^+$ observed with 9.0σ in multidimensional amplitude fit. Quantum numbers $J^P = 3/2^-$
- $P(4450)_c^+$ observed with 12.0σ in multidimensional amplitude fit. Quantum numbers $J^P = 5/2^+$

$Z(4430)^+$

- Existence confirmed with $> 13.0\sigma$ in multidimensional amplitude fit and with $> 8.0\sigma$ in model independent analysis.
- Quantum numbers determined $J^P = 1^+$.
- Resonant behavior observed.

Summary

Will benefit from Run II statistics

$$P(4380)_c^+ \text{ and } P(4450)_c^+$$

- Resonance behavior observed for $P(4450)_c^+$, but Argant plot not conclusive for $P(4380)_c^+$.
- Increased statistics will hopefully help to settle the resonance character of $P(4380)_c^+$.

$$Z(4430)^+$$

- Evidence of a second state with reported in the amplitude fit, but not observed in model independent analysis. Argant plot not conclusive.
  - Fitted parameters:

$$M_{Z(\mathbf{4430})^{+*}} = 4239 \pm 18^{+\mathbf{45}}_{-\mathbf{10}}\ \mathrm{MeV}/c^{\mathbf{2}}, \Gamma_{Z(\mathbf{4430})^{+*}} = 220 \pm 47^{+\mathbf{108}}_{-\mathbf{74}}\ \mathrm{MeV}/c^{\mathbf{2}}$$

$$f_{Z(\mathbf{4430})^+} = (1.6 \pm 0.5^{+\mathbf{1.9}}_{-\mathbf{0.4}})\%$$

  - Significance: $\Delta(-2lnL) > 6.0\sigma$
- Higher statistics from Run II will help to settle its existence and also its resonant behavior.

Thanks!

Backup

$\Lambda_b^0 \to K^- p J/\psi$

Fit results without pentaquark states

- Fit including only Λ^* resonances, allowing all possible known states (Extended model)
- The masses and widths of the Λ^* states are fixed to their PDG values
- The m_{Kp} distribution is reasonably well fitted
- The peaking structure in $m_{J/\psi p}$ is not described

State	J^P	M_0 (MeV)	Γ_0 (MeV)	# Reduced	# Extended
$\Lambda(1405)$	$1/2^-$	$1405.1^{+1.3}_{-1.0}$	50.5 ± 2.0	3	4
$\Lambda(1520)$	$3/2^-$	1519.5 ± 1.0	15.6 ± 1.0	5	6
$\Lambda(1600)$	$1/2^+$	1600	150	3	4
$\Lambda(1670)$	$1/2^-$	1670	35	3	4
$\Lambda(1690)$	$3/2^-$	1690	60	5	6
$\Lambda(1800)$	$1/2^-$	1800	300	4	4
$\Lambda(1810)$	$1/2^+$	1810	150	3	4
$\Lambda(1820)$	$5/2^+$	1820	80	1	6
$\Lambda(1830)$	$5/2^-$	1830	95	1	6
$\Lambda(1890)$	$3/2^+$	1890	100	3	6
$\Lambda(2100)$	$7/2^-$	2100	200	1	6
$\Lambda(2110)$	$5/2^+$	2110	200	1	6
$\Lambda(2350)$	$9/2^+$	2350	150	0	6
$\Lambda(2585)$	?	$\approx$2585	200	0	6

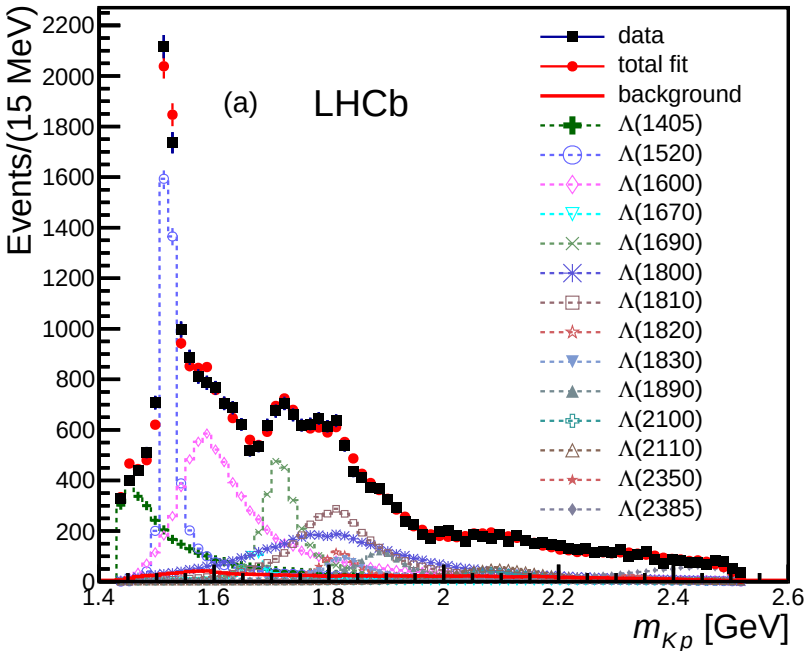

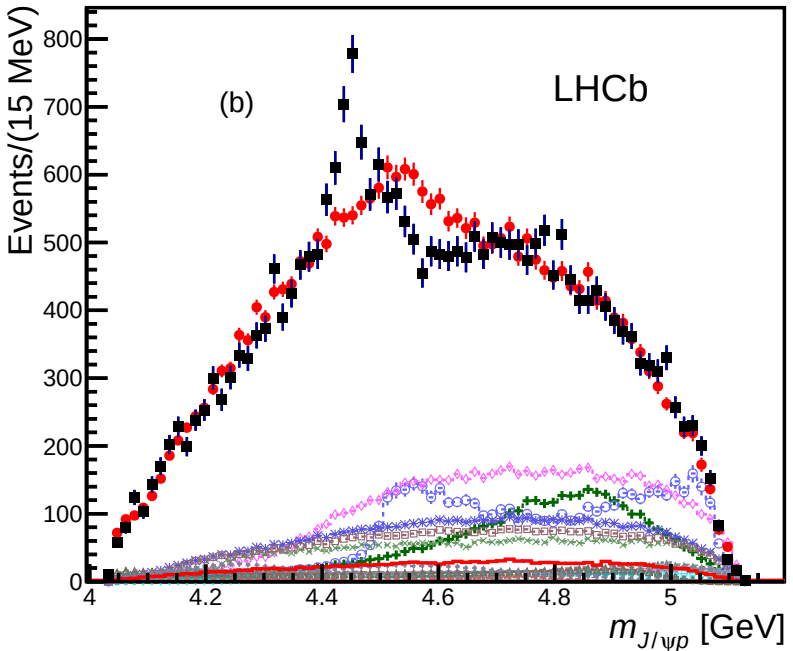

$\Lambda_b^0 \to K^- p J/\psi$: Systematic uncertainties

Table 2: Summary of systematic uncertainties on P_c^+ masses, widths and fit fractions, and Λ^* fit fractions. A fit fraction is the ratio of the phase space integrals of the matrix element squared for a single resonance and for the total amplitude. The terms "low" and "high" correspond to the lower and higher mass P_c^+ states. The sFit/cFit difference is listed as a cross-check and not included as an uncertainty.

Source	M_0 (MeV)		Γ_0 (MeV)		Fit fractions (%)			
	low	high	low	high	low	high	$\Lambda(1405)$	$\Lambda(1520)$
Extended vs. reduced	21	0.2	54	10	3.14	0.32	1.37	0.15
Λ^* masses & widths	7	0.7	20	4	0.58	0.37	2.49	2.45
Proton ID	2	0.3	1	2	0.27	0.14	0.20	0.05
$10 < p_p < 100$ GeV	0	1.2	1	1	0.09	0.03	0.31	0.01
Nonresonant	3	0.3	34	2	2.35	0.13	3.28	0.39
Separate sidebands	0	0	5	0	0.24	0.14	0.02	0.03
J^P $(3/2^+, 5/2^-)$ or $(5/2^+, 3/2^-)$	10	1.2	34	10	0.76	0.44		
$d = 1.5 - 4.5$ GeV^{-1}	9	0.6	19	3	0.29	0.42	0.36	1.91
$L^{P_c}_{\Lambda_b^0}$ $\Lambda_b^0 \to P_c^+$ (low/high)K^-	6	0.7	4	8	0.37	0.16		
L_{P_c} P_c^+ (low/high) $\to J/\psi p$	4	0.4	31	7	0.63	0.37		
$L^{\Lambda_n^*}_{\Lambda_b^0}$ $\Lambda_b^0 \to J/\psi \Lambda^*$	11	0.3	20	2	0.81	0.53	3.34	2.31
Efficiencies	1	0.4	4	0	0.13	0.02	0.26	0.23
Change $\Lambda(1405)$ coupling	0	0	0	0	0	0	1.90	0
Overall	29	2.5	86	19	4.21	1.05	5.82	3.89
sFit/cFit cross check	5	1.0	11	3	0.46	0.01	0.45	0.13

$\Lambda_b^0 \to K^- p J/\psi$: Slices $m_{pJ/\psi}$

Figure 8: $m_{J/\psi p}$ in various intervals of m_{Kp} for the fit with two P_c^+ states: (a) $m_{Kp} < 1.55$ GeV, (b) $1.55 < m_{Kp} < 1.70$ GeV, (c) $1.70 < m_{Kp} < 2.00$ GeV, and (d) $m_{Kp} > 2.00$ GeV. The data are shown as (black) squares with error bars, while the (red) circles show the results of the fit. The blue and purple histograms show the two P_c^+ states. See Fig. 7 for the legend.

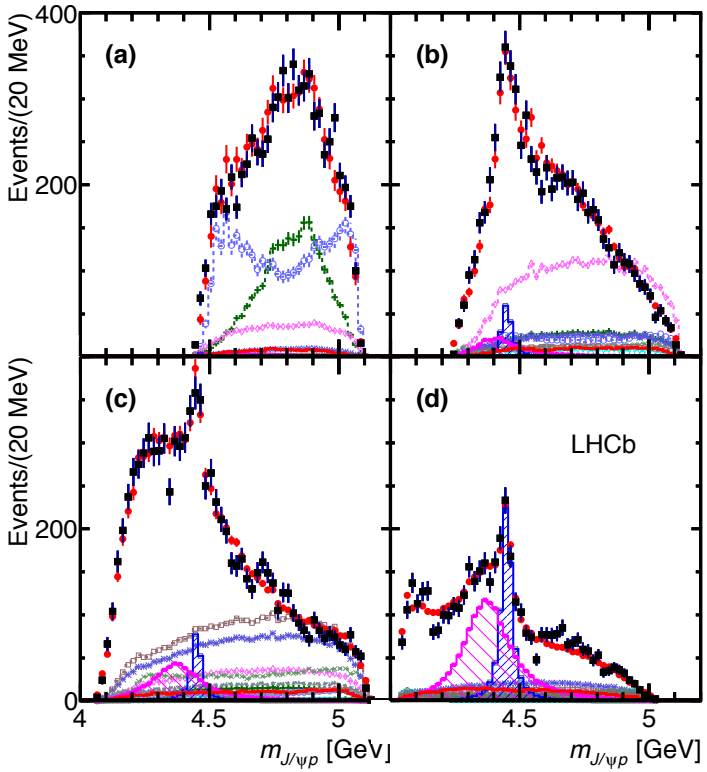

$\Lambda_b^0 \to K^- p J/\psi$: Slices $m_{KJ/\psi}$

Figure 11: Projections onto $m_{J/\psi K}$ in various intervals of m_{Kp} for the reduced model fit (cFit) with two P_c^+ states of J^P equal to $3/2^-$ and $5/2^+$: (a) $m_{Kp} < 1.55$ GeV, (b) $1.55 < m_{Kp} < 1.70$ GeV, (c) $1.70 < m_{Kp} < 2.00$ GeV, (d) $m_{Kp} > 2.00$ GeV, and (e) all m_{Kp}. The data are shown as (black) squares with error bars, while the (red) circles show the results of the fit. The individual resonances are given in the legend.

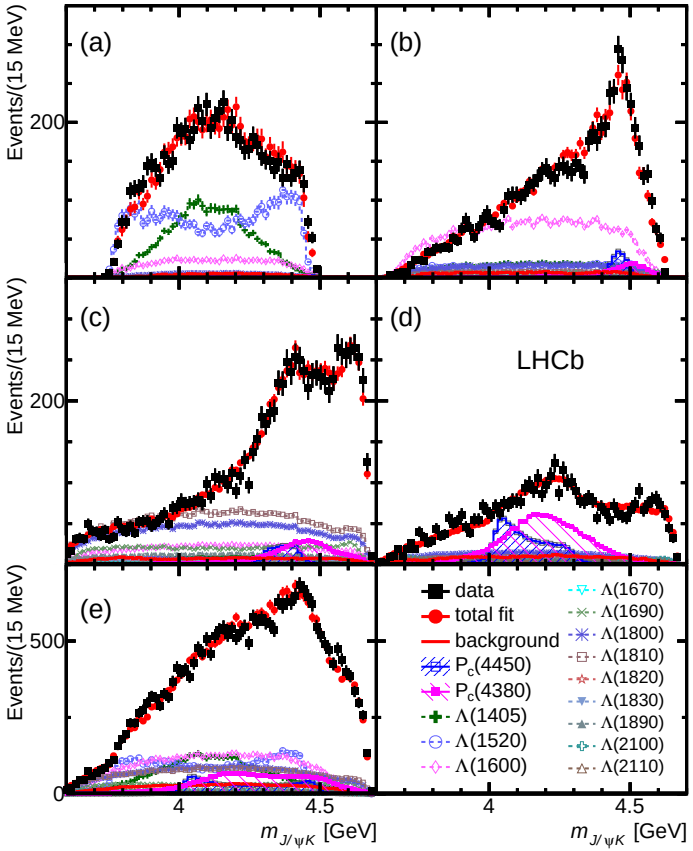

$Z(4430)^+$

- Charged charmonium like state reported by Belle in $B^0 \to \psi(2S)K^+\pi^-$ decays [Phys.Rev.D88:074026]
- Searched and not confirmed or excluded by BaBar [Phys.Rev.D79:112001]
- Can not be explained as conventional meson.
- Minimum quark content: $c\bar{c}u\bar{d}$
- No corresponding structure observed in $B^0 \to J/\psi K^+\pi^-$

$Z(4430)^+$ at Belle. K^{*0} and $K_2^*(1432)$ vetoed.

With $Z(4430)^+$ and No $Z(4430)^+$

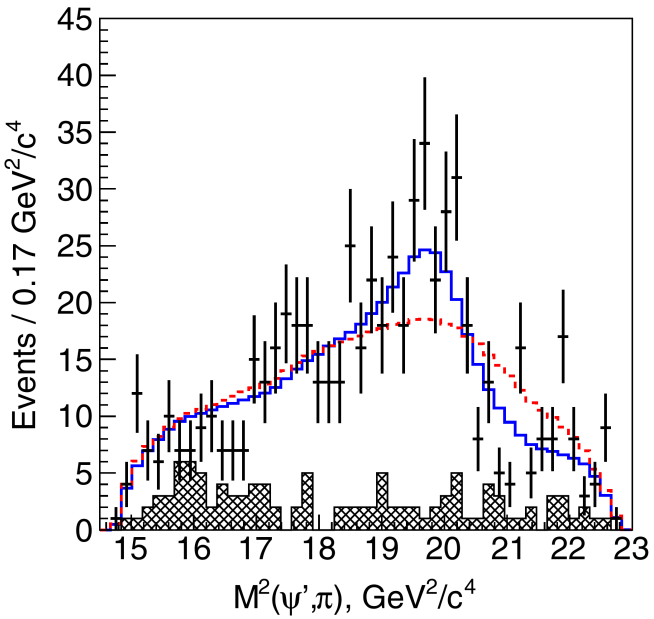

$Z(4430)^+$ at BaBar. Legendre polynomials approach.

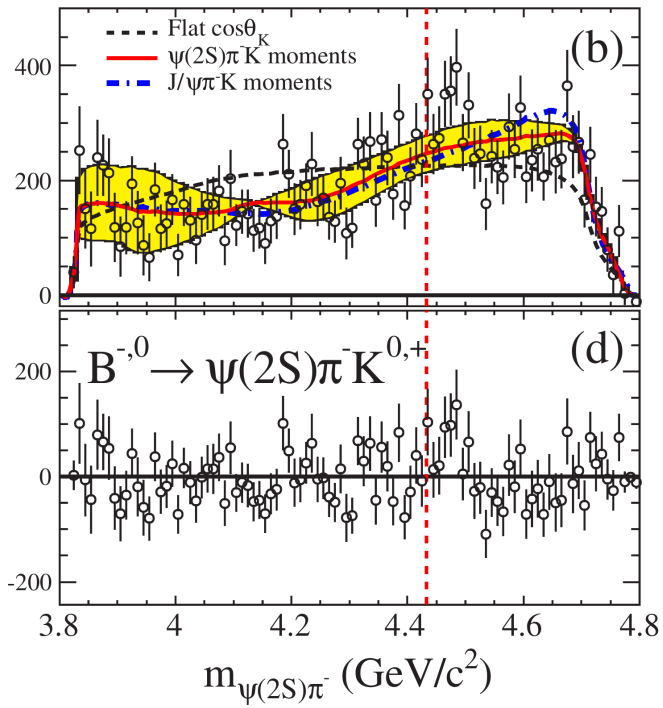

$Z(4430)^+$: model independent analysis

Phys. Rev. D 92, 112009 (2015)

The main goal is to check if the structures in the $\mathrm{m}_{\psi(2S)\pi}$ spectrum can be explained as reflections of the resonance activity in the $\mathrm{K}\pi$ system.

- No assumptions on the shape and coupling of the K^* resonances.
- Only its maximum J is restricted.

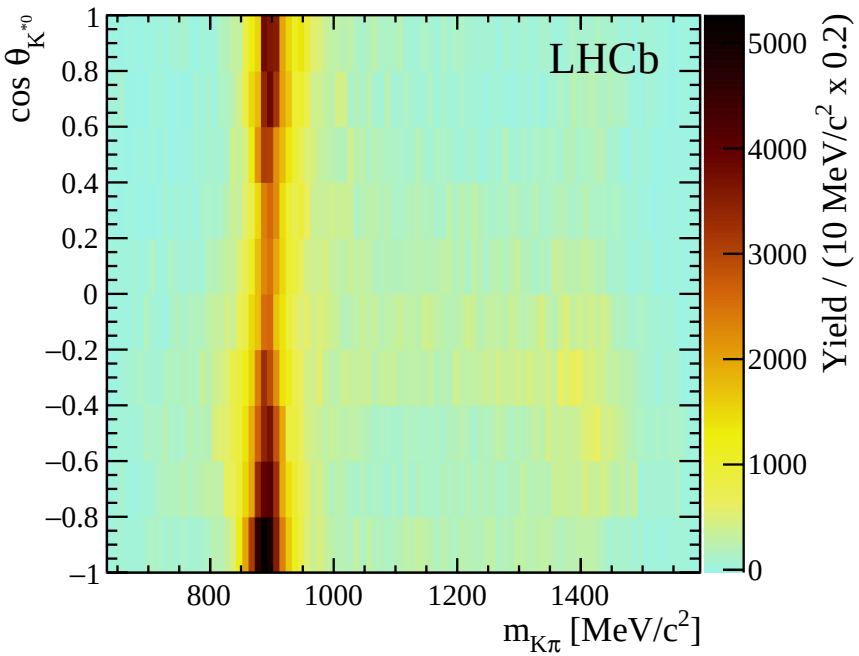

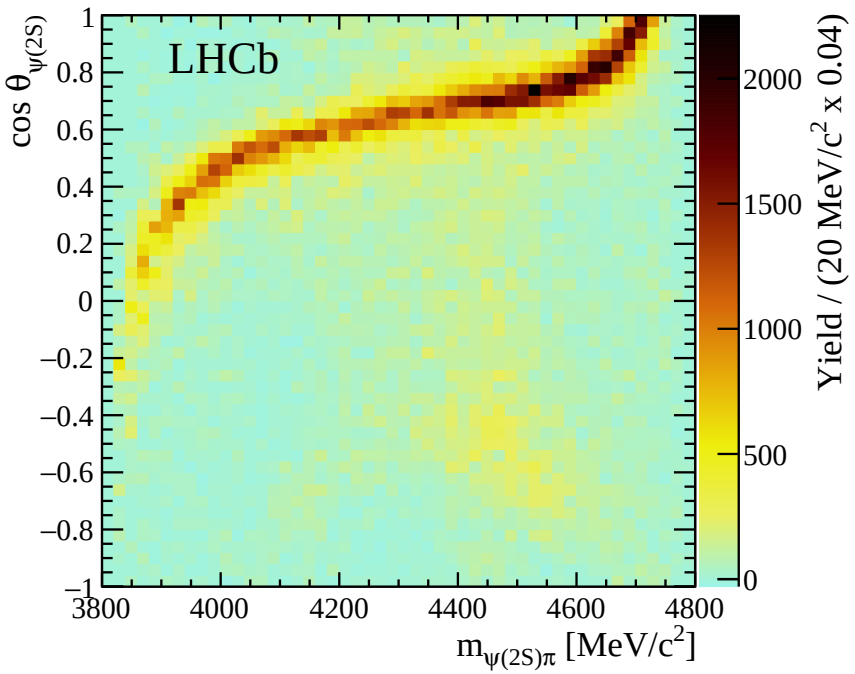

$Z(4430)^+$: model independent analysis

Slices of $m_{K\pi}$

Toy Monte Carlo prediction in slices of $m_{K\pi}$.

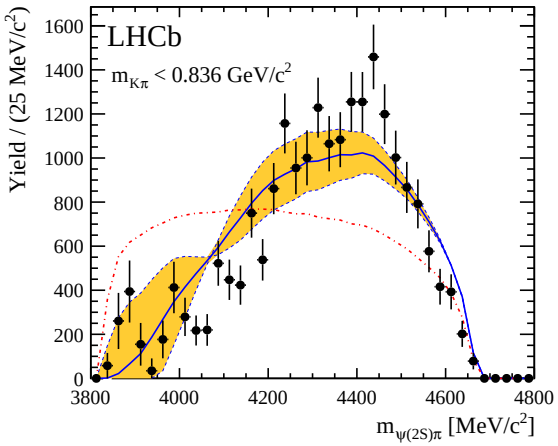

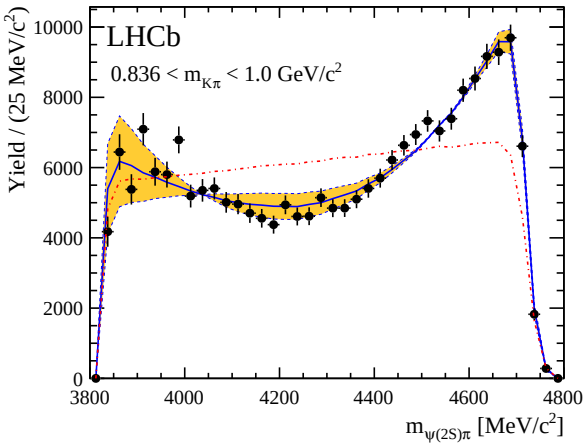

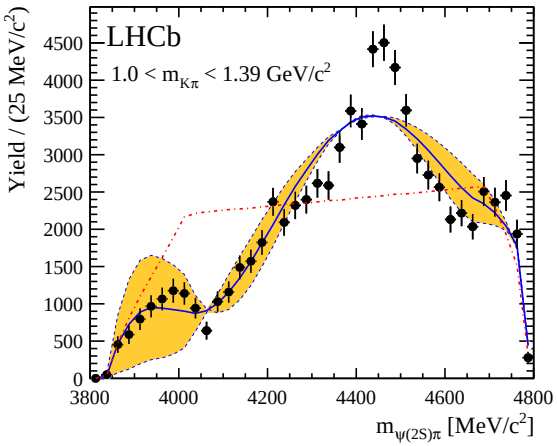

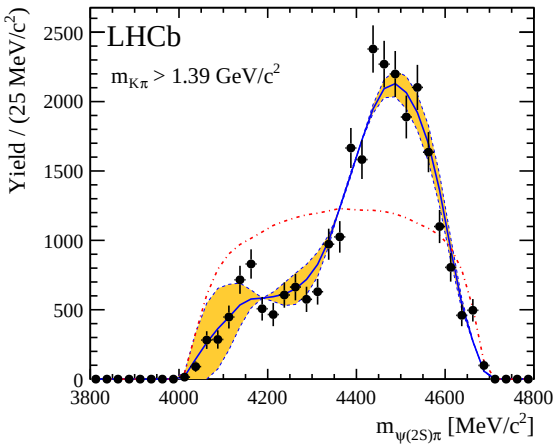

- **Data points(black dots)**
- **MC prediction (blue solid line)**
- Phase space MC weighted to reproduce $m_{K\pi}$ (red line)
- Clear disagreement between data and MC on the slice $1.0 < m_{K\pi} < 1.39\,\mathrm{GeV}/c^2$

$Z(4430)^+$: model independent analysis

Additional studies: $l_{max} \leq 4$

- Setting the maximum Legendre polynomial order to four, independent of $\mathrm{m_{K\pi}}$
- This corresponds to suppose the $\mathrm{K\pi}$ system has S,P and D waves contributing in all regions.
- Data can not be reproduced

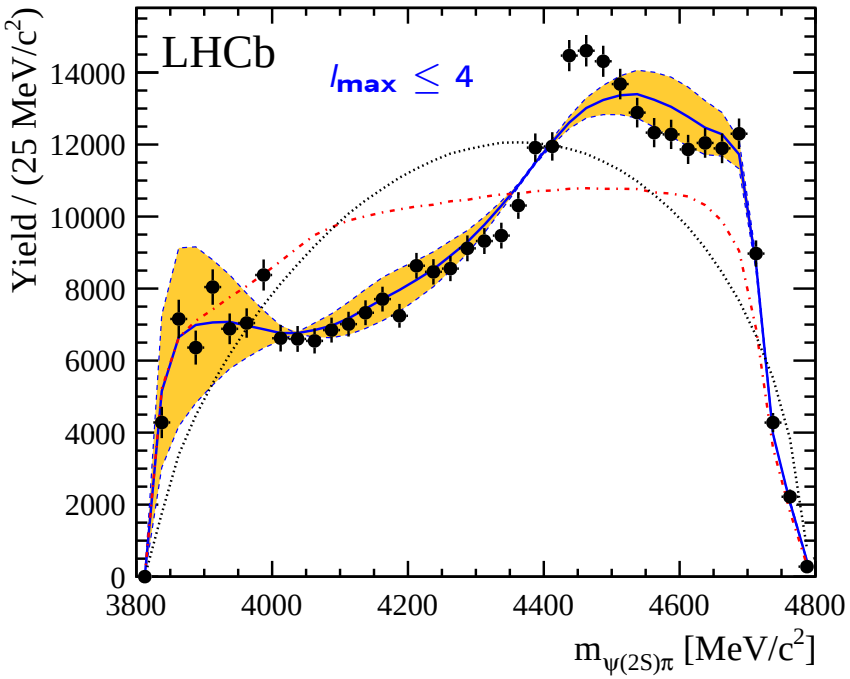

full $\mathrm{m_{K\pi}}$ spectrum

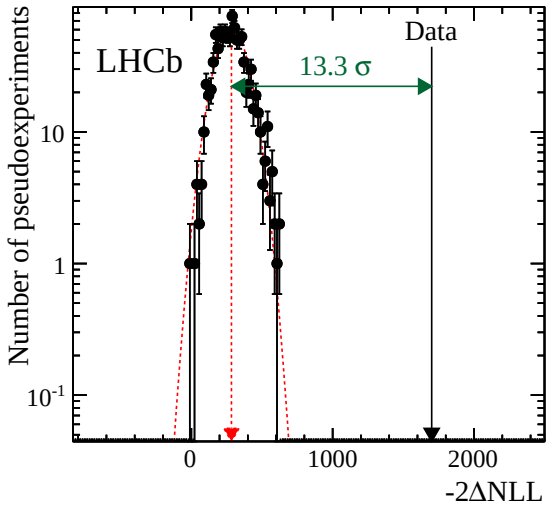

$1.0 < \mathrm{m_{K\pi}} < 1.39\ \mathrm{GeV}/c^2$

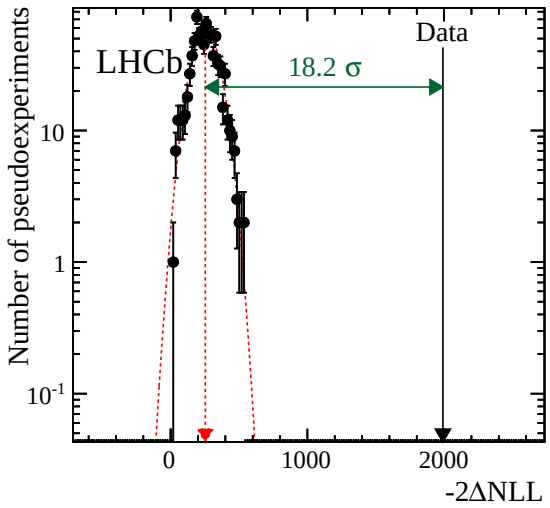

$Z(4430)^+$: model independent analysis

Additional studies: $l_{max} \leq 6$

- Setting the maximum Legendre polynomial order to six, independent of $\mathrm{m_{K\pi}}$
- This corresponds to suppose the $\mathrm{K\pi}$ system has S, P, D and F waves contributing in all regions.
- Data still can not be reproduced

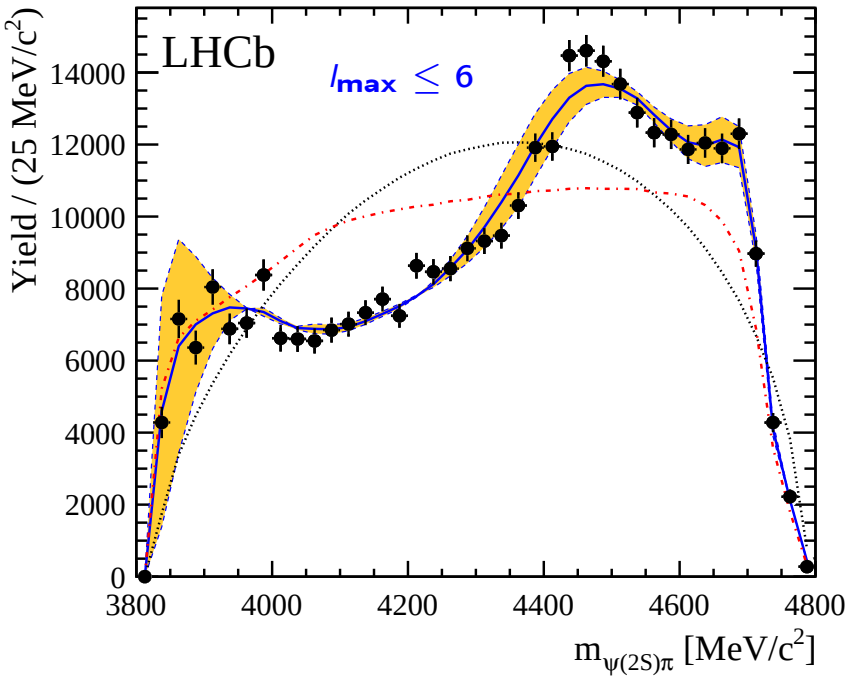

full $\mathrm{m_{K\pi}}$ spectrum

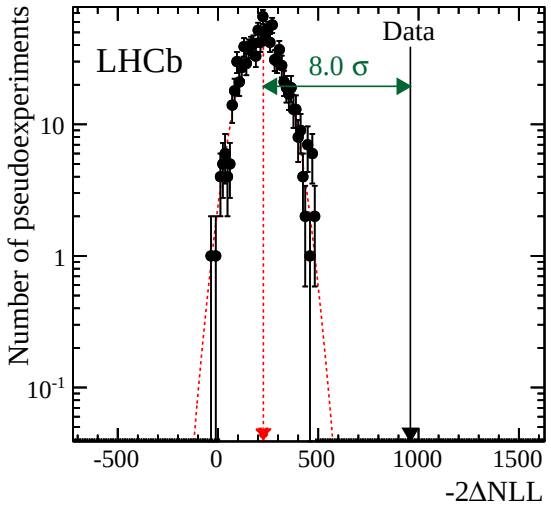

$1.0 < \mathrm{m_{K\pi}} < 1.39\ \mathrm{GeV}/c^2$